MURATAITE, A UB$_{12}$ DERIVATIVE STRUCTURE WITH CONDENSED KEGGIN MOLECULES

T. SCOTT ERCIT

Research Division, Canadian Museum of Nature, Ottawa, Ontario K1P 6P4

FRANK C. HAWTHORNE

Department of Geological Sciences, University of Manitoba, Winnipeg, Manitoba R3T 2N2

ABSTRACT

The crystal structure of murataite, space group $F\bar{4}3m$, a 14.886(2) Å, has been solved by Patterson methods and refined to an R of 4.91 (wR 4.71%) for 265 observed reflections (MoKα radiation). The ideal formula is $(Y,Na)_6(Zn,Fe)_5Ti_{12}O_{29}(O,F)_{10}F_4$ with $Z = 4$, but its simple appearance conceals extensive cation disorder within the structure. There are four distinct cation sites: the X site is [8]-coordinated and contains $(Y,HREE,Na,Ca,Mn)$; the T site is tetrahedrally coordinated and contains (Zn,Si); the $M1$ site is octahedrally coordinated and contains (Ti,Nb,Na); the $M2$ site is [5]-coordinated by a triangular bipyramid and contains (Zn,Fe^{3+},Ti,Na). Three $M1$ octahedra share edges to form a compact $M_3\phi_{13}$ group. Four of these $M_3\phi_{13}$ groups link by sharing corners to form a tetrahedral cage in the center of which is the T site. The resulting Keggin-structured $[M_{12}T\phi_{40}]^{n-}$ unit may be considered as the fundamental building block of the structure. The net formed by linkage of the $M1$ polyhedra is topologically the same as the B net of UB$_{12}$, which accounts for the similarity of X-ray properties of murataite and this compound.

Keywords: murataite, crystal structure, Ti-oxide mineral, rare-earth elements, peralkaline granitic pegmatite, Keggin structure, UB$_{12}$.

SOMMAIRE

Nous avons affiné la structure cristalline de la murataïte, groupe spatial $F\bar{4}3m$, a 14.886(2) Å, par méthodes de Patterson jusqu'à un résidu R de 4.91 (wR 4.71%) en utilisant 265 réflexions observées (rayonnement MoKα). La formule idéale, $(Y,Na)_6(Zn,Fe)_5Ti_{12}O_{29}(O,F)_{10}F_4$ avec $Z = 4$, semble assez simple, mais elle recèle un désordre important impliquant les cations. Ils occupent quatre sites distincts: le site X a une coordinence huit et contient $(Y,HREE,Na,Ca,Mn)$. Le site T, à coordinence quatre, contient (Zn,Si). Le site $M1$ a une coordinence octaédrique et contient (Ti,Nb,Na), et le site $M2$ a une coordinence cinq, entouré d'une bipyramide triangulaire contenant (Zn,Fe^{3+},Ti,Na). Trois octaèdres partagent une arête pour former un agencement compact à stoechiométrie $M_3\phi_{13}$. Quatre de ces groupes $M_3\phi_{13}$, liés par partage de coins, forment une cage tétraédrique dont le centre est occupé par le site T. Il en résulte un agencement $[M_{12}T\phi_{40}]^{n-}$ à structure de Keggin, que nous considérons le bloc structural fondamental de la charpente. Le réseau résultant de l'agencement des polyèdres $M1$ est topologiquement le même que celui des atomes B du composé UB$_{12}$, ce qui rend compte de la ressemblance des spectres de diffraction X de la murataïte et de ce composé.

(Traduit par la Rédaction)

Mots-clés: murataïte, structure cristalline, oxyde de Ti, terres rares, pegmatite granitique hyperalcaline, structure de Keggin, UB$_{12}$.

INTRODUCTION

Understanding the crystal chemistry of (Y,REE)-bearing Ti-oxide minerals is a challenging problem. As mineralogical garbage baskets to their host granitic pegmatites or carbonatites, they are geochemically promiscuous, and from the viewpoint of structural crystallography, site assignments are difficult. The minerals commonly contain U and Th, and hence can be metamict; heating experiments commonly result in polymineralic mixtures (Ewing & Ehlmann 1974). Furthermore, if heating experiments result in a monomineralic product, there is so little information on natural, nonmetamict examples of the species that it is generally not possible to discern whether the original structure or a polymorph has been generated.

Murataite is a (Y,Ti)-oxide mineral first described by Adams *et al.* (1974) from a peralkaline granitic pegmatite in the St. Peters Dome area, Colorado. On the basis of precession photographs and results of a

chemical analysis, these authors proposed the formula $(Na,Y,Er)_4(Zn,Fe)_3(Ti,Nb)_8O_{16}(F,OH)_4$, possible space-groups $F432$, $Fm3m$ or $Fm3$, a 14.863(5) Å, $Z = 8$. Murataite is typical of (Y,Ti)-oxide minerals in terms of its complex chemical composition; however, murataite does not contain U and Th, and its crystallinity is intact. Thus a structural study of murataite can provide information on the structural crystallography of natural (Y,Ti)-oxide minerals, with particular emphasis on the degree of order among cations.

EXPERIMENTAL

We obtained the sample of murataite from the Royal Ontario Museum (catalogue number M34933). A rounded fragment was used in a preliminary precession study, which confirmed $F\overline{4}3m$ diffraction-symmetry for the mineral, giving $F\overline{4}3m$, $F432$ or $Fm3m$ as possible space-groups, a modification of the conclusion of Adams *et al.* (1974).

Collection of X-ray intensity-data

Intensity data were collected with a Nicolet $R3m$ four-circle diffractometer using the experimental method of Ercit *et al.* (1986). Twenty-five intense reflections (to a 2θ of 30°) were used to center the crystal; least-squares refinement of the setting angles gave the orientation matrix used for data collection and the unit-cell edge given in Table 1. One octant of reciprocal space (six asymmetric units) was collected to a $2\theta_{max}$ of 60°. The data were empirically corrected for absorption using a φ-scan calibration data-set ($R[merge] = 1.7\%$ after correction). Data reduction (correction for Lorentz, polarization and background effects) was done with the SHELXTL PC system of programs; the reflections were merged ($R = 2.7\%$) to give the numbers shown in Table 1.

Chemical analysis

After the collection of X-ray intensity data, the crystal was mounted in epoxy for chemical analysis by

TABLE 1. MISCELLANEOUS INFORMATION FOR MURATAITE

a (Å):	14.886(2)	Crystal radius (mm):	0.105
Space group:	$F\overline{4}3m$	Total no. of $|F_0|$:	294
Z:	4	No. of $|F_0| > 3\sigma(I)$:	265
μ (cm^{-1}, MoKα):	123	Final R (obs)%:	4.91
		Final wR (obs)%:	4.71

$X_6T_1M_{24}M1_{12}O_{29}(O,F,OH)_{10}F_4$ *, where

$X = 2.24$ Y, 1.14 HREE, 2.08 Na, 0.33 Ca, 0.21 Mn
$T = 0.89$ Zn, 0.11 Si
$M2 = 1.92$ Zn, 1.01 Fe^{3+}, 0.62 Na, 0.45 Ti
$M1 = 9.16$ Ti, 1.57 Nb, 1.27 Na
$O = 30.88$, OH = 1.23, F = 7.55

$R = \Sigma(|F_0|-|F_C|)/\Sigma|F_0| \quad wR = [\Sigma w(|F_0|-|F_C|)^2/\Sigma w|F_0|^2]^{1/2}, \ w = 1$

* basis of 23 cations

TABLE 2. CHEMICAL COMPOSITION OF MURATAITE

Composition (wt.%)		Formula Contents per 23 Cations	
Na$_2$O	6.10	Na	3.97
CaO	0.91	Ca	0.33
MnO	0.75	Mn	0.21
ZnO	11.32	Zn	2.81
Fe$_2$O$_3$	3.99	Fe^{3+}	1.01
Y$_2$O$_3$	12.53	Y	2.24
Gd$_2$O$_3$	0.27	Gd	0.03
Tb$_2$O$_3$ *	0.16	Tb	0.02
Dy$_2$O$_3$	2.59	Dy	0.28
Ho$_2$O$_3$	0.95	Ho	0.10
Er$_2$O$_3$	2.83	Er	0.30
Tm$_2$O$_3$	0.45	Tm	0.05
Yb$_2$O$_3$	3.11	Yb	0.32
Lu$_2$O$_3$	0.47	Lu	0.05
TiO$_2$	38.07	Ti	9.61
SnO$_2$	0.27	Sn	0.04
Nb$_2$O$_5$	10.10	Nb	1.53
SiO$_2$	0.34	Si	0.11
F	7.11		23.00
H$_2$O †	0.55		
O=F	-2.99	F	7.55
	99.88	OH	1.23
		O	32.11
			29.66

* interpolated;   † from Adams *et al.* (1974).

electron microprobe, a JEOL 733 instrument with Tracor Northern 5500 and 5600 automation. The accelerating potential was 15 kV, and the beam current, 20 nA. The beam diameter of 20 μm was selected to minimize migration or volatilization of Na. Standards were NaInSi$_2$O$_6$ (NaKα), microlite (CaKα), tephroite (MnKα), synthetic zincite (ZnKα), almandine (FeKα, SiKα), YAG (YLα), end-member synthetic $REPO_4$ compounds [$L\alpha$ lines for even-numbered rare-earth elements (REE), except $L\beta$ for Dy], synthetic REE-bearing glass (odd-numbered REE, all $L\alpha$, except $L\beta$ for Ho), rutile (TiKα), cassiterite (SnLα), synthetic manganocolumbite (NbLα) and NaMoO$_3$F (FKα). Overlap corrections were calculated for the REE, for ZnLα – NaKα interference, and for NbLα – YLα interference. Because of significant errors in the reduction of TiKα data with a conventional ZAF routine, a PAP algorithm (Pouchou & Pichoir 1991) in XMAQNT version 1.5 (C. Davidson, CSIRO, pers. comm.) was used for data reduction. The result given in Table 2 is very similar to the composition of the type material (Adams *et al.* 1974).

Structure solution

Structure solution and refinement were done with SHELXTL PC. Early sharpened-Patterson maps showed that most (if not all) atoms are on special positions. After considerable interpretation of the map, four cation sites and some anion sites were identified. Refinement of this early model and the generation of difference-Fourier maps showed the remaining anion sites. As the cation-site multiplicities did not obviously correspond to any groupings of cations according to the

chemical analysis, we concluded early in the refinement that there was substantial disorder among cations (multiply-occupied sites). After testing several models, we arrived at a preliminary result with one (Y,Na) site (X), one Ti site (M1), one Zn site (M2), and one Fe site (T).

Structure refinement

At this stage, the basic atomic arrangement was in place; however, final elucidation of the degree of cation order was an extremely demanding task that warrants detailed discussion. Specifically, the final pattern of cation order in murataite, a nonmetamict rare-earth-oxide mineral, gives considerable insight into the type of initial patterns of cation order that probably occurred in now-metamict rare-earth-oxide minerals prior to the metamictization process.

Problems with the initial model were as follows: (1) there is much more (Na + Y) than the X site can accommodate; (2) difference-Fourier maps showed that if all (Y + REE) is assigned to the X site and the remainder of the site assigned as Na, there is still significant residual density at the site, indicating that even heavier constituents at X are required; (3) as the assignment of neither Ti to M1 nor Zn to M2 seemed to be wrong, and as none of the difference-Fourier maps showed evidence of an additional cation site, Na *must* be disordered over several sites; (4) bond-valence sums favored the occurrence of Zn at the T site, and a mixture of Zn and Fe^{3+} at the M2 site. Given these observations, several models are possible. The most ordered, crystal-chemically sensible of these places Y + REE and most Na at X, Ti and minor Na at M1, Zn, Fe and minor Na at M2, and Zn and minor Si at T; this model converged to R = 5.4, wR = 5.5%. The most disordered model, least-feasible in crystal-chemical terms, has Y, Na and Ti at X, Ti and Na at M1, Zn, Fe and minor Na at M2, and Zn and minor Si at T; this converged to R = 4.6, wR = 4.5%. The latter model is clearly superior to the first in matching the scattering from the various sites. However, neither of the models match expectations on the basis of bond-valence sums. For the more ordered model, the observed sum at the X site is 0.35 v.u. higher than expected, whereas for the disordered model, the observed sum at the X site is 0.85 v.u. lower than expected; in addition, the Ti site is 0.49 v.u. higher than expected. Consequently, an intermediate model was adopted to minimize the differences between observed and expected bond-valence sums for the various cation sites; this model converged to R = 5.1, wR = 5.1%.

On the basis of both the displacement parameters and difference-Fourier maps, it was apparent in early stages of refinement that O4 and F are positionally disordered. Difference-Fourier maps show that O4 is displaced from its 4d site, and that F is displaced from the threefold axis of its 16e site, each to partly occupied

48h sites. A problem in stoichiometry was also noticed, as the structure analysis indicates that there are 43 anions per formula unit, whereas the formula calculated from the results of the chemical analysis gives a maximum of 39.7 anions (for a normalization basis of 23 cations per formula unit [*pfu*]). As the final difference-Fourier map does not indicate the presence of any other cation sites, this finding supports the basis of normalization and demonstrates that vacancies are present at the anion sites in the structure. In an attempt to determine whether these vacancies are ordered, we simultaneously refined the occupancies of all anion sites while keeping the site occupancies of the cations fixed. All sites had refined occupancies within two standard deviations of ideal, except for O2. The occupancy of O2 was six standard deviations lower than ideal, yet close (three standard deviations) to the value expected if all vacancies occur at O2; we thus conclude that the anion deficiency is localized at the O2 site.

The final refinement, incorporating all of the features listed above, converged to R = 4.91, wR = 4.71% (R = 5.25, wR = 4.81% for all 294 data). The observed and calculated structure-factors are available from the Depository of Unpublished Data, CISTI, National Research Council of Canada, Ottawa, Ontario K1A 0S2.

RESULTS AND DISCUSSION

Positional and displacement parameters for the murataite structure are given in Table 3, bond lengths in Table 4, bond angles and polyhedral edge-lengths in Table 5, and bond valences in Table 6.

Anion ordering and anion coordination

As cation site-occupancies were assigned in a large part according to bond-valence sums, the sums of the

TABLE 3. POSITIONAL AND DISPLACEMENT PARAMETERS FOR MURATAITE

	x	y	z	U_{eq}
X	0.1812(2)	0	0	74(5)
M1	0.1629(2)	0.1629(2)	0.5087(4)	80(7)
M2	-0.1722(2)	-0.1722(2)	-0.1722(2)	65(6)
T	1/2	1/2	1/2	135(18)
O1	0.2976(8)	0.0729(6)	0.0729(6)	85(23)
O2*	0.3962(8)	0.3962(8)	0.742(1)	100
O3	0.5738(9)	0.5738(9)	0.5738(9)	56(43)
O4	1/4	1/4	0.767(5)	100
O5	0.015(1)	1/4	1/4	132(36)
O6	-0.079(1)	-0.079(1)	-0.079(1)	116(44)
F	0.106(1)	0.106(1)	0.085(2)	100

	U_{11}	U_{22}	U_{33}	U_{23}	U_{13}	U_{12}
X	64(13)	79(7)	79(7)	11(12)	0	0
M1	72(9)	72(9)	95(18)	-14(8)	-14(8)	-1(10)
M2	65(10)	65(10)	65(10)	20(10)	20(10)	20(10)

All U values are $Å^2$ x 10^4; U values for O2, O4 and F are constrained at 0.01 $Å^2$. Displacement parameters are of the form: $exp[-2\pi^2(U_{11}h^2a^{*2} + U_{22}k^2b^{*2} + ... 2U_{12}hka^*b^*)]$.
* Refined occupancy of O2 = 0.82(3)

TABLE 4. BOND LENGTHS (Å) IN MURATAITE

X-O1 x 2	2.32(1)	$M1$-O1 x 2	1.902(5)	$M2$-O2 x 3	1.93(2)
-O2 x 2	2.47(2)	-O2 x 2	2.039(10)	-O4 x 1/2	1.87(4)
-O6 x 2	2.251(6)	-O3	2.111(11)	-O4 x 1/2	2.17(5)
-F x 4/3	2.32(1)	-O5	1.867(5)	-O6	2.41(3)
-F x 2/3	2.66(3)	<$M1$-O>	1.977	<$M2$-O>	2.04
<X-ϕ>	2.37				

T-O3 x 4   1.90(2)

TABLE 5. SELECTED INTRAPOLYHEDRAL ANGLES (°) AND DISTANCES (Å)
          IN MURATAITE

O1-X-O2 x4	69.6(3), 2.73(2)	O1-$M1$-O1	91.5(7), 2.73(2)
-F	77.4(7), 2.89(2)	-O2 x2	87.8(6), 2.73(2)
-F	80.9(6), 3.24(3)	-O3 x2	92.6(5), 2.91(1)
O2-X-O6 x2	70.4(7), 2.73(2)	-O5 x2	98.9(6), 2.86(1)
O6-X-F x4/3	68.6(4), 2.79(2)	O2-$M1$-O2	90.9(9), 2.90(3)
-F x4/3	66.6(5), 2.51(3)	-O3 x2	76.8(5), 2.58(2)
-F x4/3	75.2(7), 2.79(2)	-O5 x2	91.7(6), 2.81(1)
<ϕ-X-ϕ>	71.5	<O-$M1$-O>	89.8
<ϕ-ϕ>	2.77	<O-O>	2.78

O3-T-O3 x6	109.5(0), 3.11(4)	O2-$M2$-O2 x3	115.0(4), 3.25(3)
		-O4	106(1), 3.27(6)
		-O4	100(1), 2.90(5)
		-O4 x1/2	97(2), 3.08(2)
		-O4 x1/2	110(2), 3.10(2)
		-O6 x3	76.9(5), 2.73(2)
		<O-$M2$-O>	98.4
		<O-O>	3.02

TABLE 6. BOND-VALENCE TABLE FOR MURATAITE

	O1	O2	O3	O4	O5	O6	F	SUM
X	0.36	0.24				0.43	0.27	2.47
							0.12	
$M1$	0.78	0.55	0.46		0.85			3.96
$M2$		0.58		0.67		0.17		2.39
				0.31				
T			0.55					2.20
SUM	1.91	1.91	1.93	1.97	1.70	1.45	0.66	

Expected sums from site assignments: X 2.22, $M1$ 3.81, $M2$ 2.32, T
2.23 v.u. Bond valences (v.u.) from curves of Brown (1981) and
Ercit (1986).

cation sites match the expected formal valences well.
The bond-valence sums at the anion sites show the
F site to be solely occupied by F, and the O1 to
O4 sites, by O. As the F site accommodates only four
anions *pfu*, the remaining 4.8 (F + OH) must occupy
other anion sites. The obvious candidates are O5 and
O6, which accommodate six and four anions *pfu*,
respectively. The bond-valence sums to these sites
indicate that the (F + OH) is disordered over both
sites, with a preference for O6. The monovalent anion
content of O5 and O6, assuming no significant
hydrogen bonding by OH groups, is approximated as
$6 \times (2 - 1.70) + 4 \times (2 - 1.45) = 4.0$ anions *pfu*,
reasonably similar to the expected value of 4.8 anions
pfu.

Positional disorder of the F anion results in the
following changes: instead of coordination of F by
three Y atoms at 2.42 Å, F is coordinated by two
Y atoms at 2.32 Å and one Y atom at 2.66 Å. Similarly,
positional disorder of the O4 anion results in
degeneracy of the $M2$–O4 bond from 2.00 Å to equal
numbers of bonds at 1.87 and 2.17 Å. Both changes in
geometry result in improved bond-valence sums to the
anions; positional disorder of the anions would seem to
be driven by bond-valence requirements of the anions.

Coordination polyhedra

An asymmetric unit of coordination polyhedra is
shown in Figure 1. The $X\phi_8$ polyhedron is a distorted
cube with a <X–ϕ> distance of 2.37 Å (where ϕ
represents O,F,OH). The TO_4 polyhedron is an ideal
tetrahedron with T_d symmetry. The average geometry
of the $M2$ site is [5]-coordination; the $M2O_5$ poly-
hedron is a distorted trigonal bipyramid with equatorial
O2 anions and with apical O6 and O4 anions. Most of
the distortion of the $M2O_5$ bipyramid is associated with
the discrepancy in length of the two apical bonds, and
a shift of the $M2$ cation out of the equatorial plane
toward O6. The $M1O_6$ polyhedron is a distorted octa-
hedron; most distortion, *e.g.*, displacement of the $M1$
cation from the geometrical center of the polyhedron
and shortening of shared edges, is associated with
Ti–Ti repulsion across shared edges.

Linkage of polyhedra

The $M1\phi_6$ octahedra share edges to form $M\phi_{13}$
trimers, which are cross-linked *via* corners to form a
complex framework. A representation of this frame-
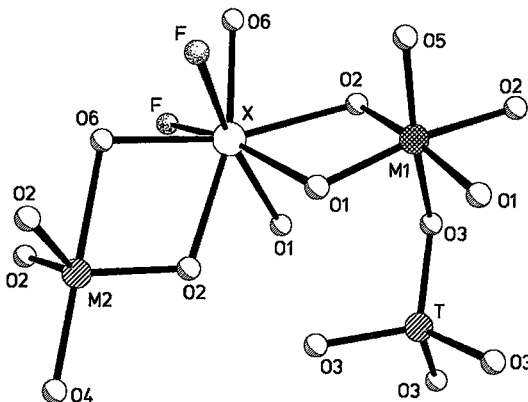
FIG. 1. An asymmetric unit of polyhedra; for clarity, only the
average positions of O4 and F are shown.
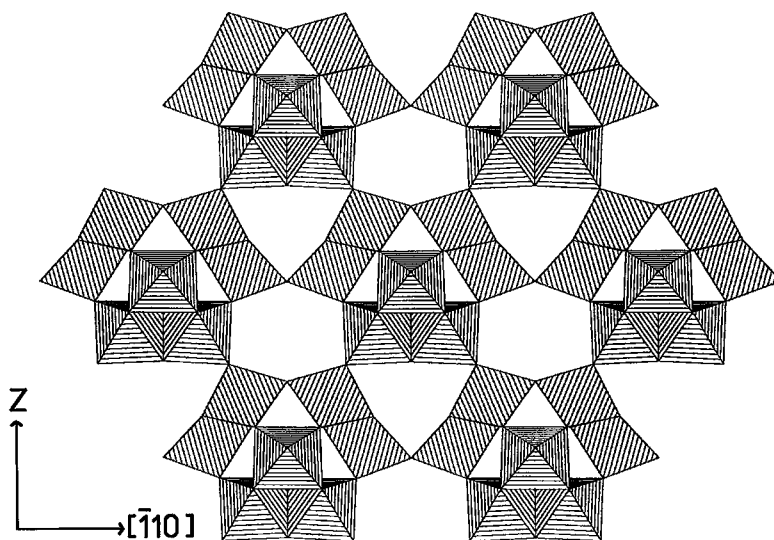
FIG. 2. Polyhedral representation of the framework of octahedra in the murataite structure ([110] projection).

work of polyhedra is shown in Figure 2, wherein the trimers and the style of corner-linking are obvious, but the three-dimensional aspects of the framework are not. Consequently, Figure 3 emphasizes the network aspect of the framework of octahedra. In Figure 3, the trimeric units are represented by the triangular circuits; all other circuits denote corner-sharing linkages. The three-dimensional net consists of three types of cage; in ascending order of size, these are: (1) a small cuboctahedron bound by circuits of three and four, which encloses one TO_4 tetrahedron; (2) a truncated tetrahedron bound by circuits of three and six; the faces with circuits of six each have one central $M2$ cation that serves to reinforce bonding within each such face; (3) a truncated octahedron bound by circuits of six and four, which encloses six X cations. The truncated octahedra that host the X cations are interconnected by edges only. This net is also common to the compound UB_{12} (Bertaut & Blum 1949), the nodes of the net denoting B atoms in the structure. The U atoms in UB_{12} are like the X cations of murataite in that they occupy the large cage of the truncated octahedron; however,

FIG. 3. Network representation of the framework of octahedra (clinographic X-axis projection).
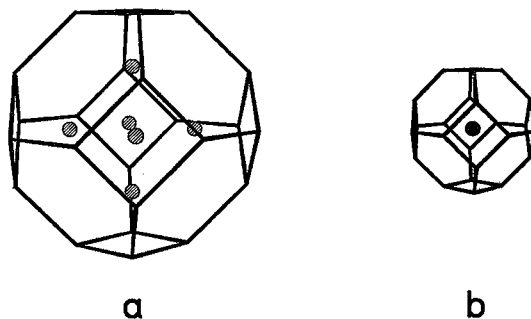
FIG. 4. Clinographic projection of the truncated octahedral cage in murataite (a) and UB_{12} (b). There are six Y atoms (shaded circles) per cage in murataite, but only one U atom per cage in the smaller-caged UB_{12}.
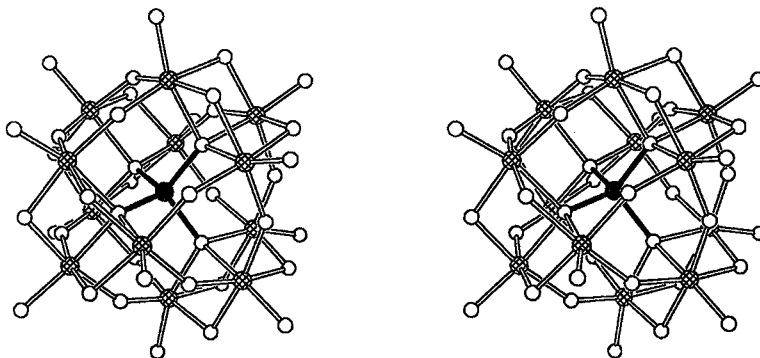
FIG. 5. Stereographic projection of the fundamental building block (*FBB*) of murataite. Cations are shown as shaded circles, and anions, as open circles; *T*–O bonds are solid, and *M*–O bonds are hollow. The *FBB* of murataite has the α form of the Keggin structure, formula $[M_{12}TO_{40}]^{n-}$.

the shorter B–B spacings of the net in UB_{12} (1.79 Å), compared to the Ti–Ti spacings for the net in murataite (average 3.6 Å), result in only one U atom per cage, located at its geometrical center (Fig. 4). This 1:2 ratio in the node spacings of the nets for UB_{12}, as compared to murataite is also reflected in their cell edges: a(murataite) ≈ $2a$(UB_{12}).

The above discussion illustrates and explains similarities in the X-ray properties of murataite and UB_{12}. However, a more suitable way of describing the fundamental building block (*FBB*) of the murataite structure is to consider all strongly bonded linkages (*e.g.*, with Pauling bond-strengths greater than 0.5 *v.u.*). The *FBB*

of murataite (Fig. 5) has a tetrahedral core surrounded by four $M_3\phi_{13}$ trimers; the resulting formula of the *FBB* is $[M_{12}T\phi_{40}]^{n-}$, ideally $[Ti_{12}ZnO_{40}]^{30-}$. The structure of this polyanion is common to many heteropoly acids of W and Mo, and to a more limited extent, of Nb, Ta and U. It is known as the *Keggin structure*. Furthermore, many isomers of the Keggin structure are known (Pope 1983); the *FBB* of murataite (Fig. 6) with its T_d symmetry has the α form. Of the many known and proposed isomers of the Keggin structure, the α form is the most stable. Murataite differs from synthetic compounds with the Keggin structure in that it consists of a condensation of Keggin molecules, hence is the only known inorganic solid with such a condensed structure.

Local (short-range) order

One of the interesting features of the murataite structure is the broad degree of disorder of cations and anions. Some of the more unusual features of the structure might owe their origin to local ordering. Two of these features are addressed below.

(1) *Na at M1*. To ensure a reasonable bond-valence sum at O3, the presence of Si at the *T* site might require Na at *M1*. For ideal murataite, with Ti at *M1* and Zn at *T*, O3 has a Pauling bond-strength sum of 3 × (4/6) + (2/4) = 2.5 *v.u.* Substitution of Si for Zn would seem unfavorable, as it increases the bond-valence sum. However, if Si substitution at *T* were coupled with Na substitution at *M1*, the bond-valence sum at O3 should remain favorably close to 2; as an extreme, complete Na + Si substitution for Ti + Zn would result in a Pauling bond-strength sum to O3 of 3 × (1/6) + (4.4) = 1.5 *v.u.* With the Keggin-structured arrangement of *M1* and *T* cations, the locally ordered model would have each Si surrounded by twelve Na atoms. The results of
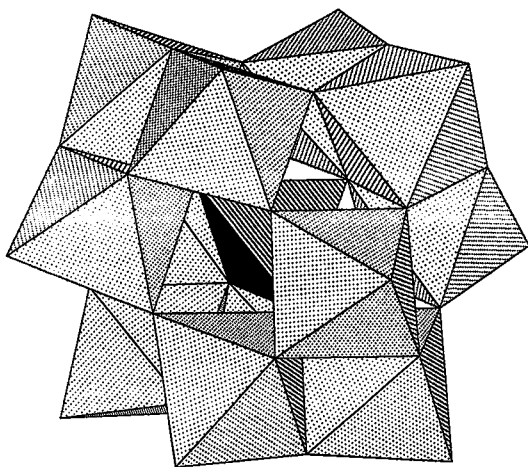
FIG. 6. Polyhedral representation of the *FBB* of murataite.

the microprobe analysis show 0.12 Si *pfu*; consequently, the model predicts 1.4 Na atoms at $M1$, in excellent agreement with the refinement (1.3 Na at $M1$).

(2) *X-site cations and coordinating anions.* With respect to X–F bonds, F disorders into positions that give two short bonds and one long bond (Table 4). This pattern is most likely associated with $2(Y + REE + Mn):1(Na + Ca)$; *i.e.*, the ratio of the number of smaller cations to larger cations. Symmetry forces 2:1 positional disorder for F, hence ⅓ occupancy of X by (Na,Ca). At a slightly more detailed level, the number of Na atoms at X exceeds the number of Na atoms at $M2$ and is approximately equal to the number of (OH,F) atoms at O6; this may indicate that Na substitution for the more highly charged (Y,REE) at X and for Zn at $M2$ may be partly accommodated by substitution of (OH,F) for O at O6.

Comparison with the structures
of other complex oxide minerals

Although the degree and style of disorder among cations in murataite might seem extreme, comparison with members of the chemically similar crichtonite group (Gatehouse *et al.* 1979) shows similarities. Indeed, the unknown phase associated with murataite, labelled "mineral Y" by Adams *et al.* (1974), has been shown by Foord *et al.* (1984) to be senaite, a member of the crichtonite group. Landauite, ideally $NaMnZn_2(Ti,Fe)_{18}O_{38}$ (Grey & Gatehouse 1978), is the member of the crichtonite group that is compositionally most similar to murataite, ideally $(Y,Na)_6(Zn,Fe)_5Ti_{12}O_{29}(O,F)_{10}F_4$. Members of the crichtonite group show (1) major amounts of Fe, Zn and Mg at the tetrahedral site, generally disordered; (2) U, Y, Mn, Fe and Zr at the $M1$ (octahedral) site; disorder here occasionally involves major amounts of small and large cations (*e.g.*, Mg and the REE in loveringite); (3) Ca, $LREE$, Pb, Na, Sr, Ba at the [12]-coordinated $M0$ site. Evidently, a variety of schemes of cation substitution and varying styles of cation disorder are the norm rather than the exception for such Ti-oxide minerals.

Betafite-subgroup minerals, which represent the Ti-dominant class of the pyrochlore group, are another highly symmetrical, framework class of Ti-oxide mineral. Because of the tunnel-like connectivity of their large-cation cages, pyrochlore-group minerals occasionally possess such exotic properties as ionic conductivity, high proportions of vacancies at the large cation site, and large cations that are easily replaced in ion-exchange experiments (Ercit *et al.* 1993). As the large cages in the structure of murataite are interconnected by edges only, we expect large-cation mobility to be severely impeded in this structure type; hence, murataite is not expected to show the exotic properties displayed by pyrochlore-group minerals.

REFERENCES

ADAMS, J.W., BOTINELLY, T., SHARP, W.N. & ROBINSON, K. (1974): Murataite, a new complex oxide from El Paso County, Colorado. *Am. Mineral.* **59**, 172–176.

BERTAUT, F. & BLUM, P. (1949): La structure des borures d'uranium. *C.R. Acad. Sci. Paris* **229**, 666–667.

BROWN, I.D. (1981): The bond-valence method: an empirical approach to chemical structure and bonding. *In* Structure and Bonding in Crystals II (M. O'Keeffe & A. Navrotsky, eds.). Academic Press, New York, N.Y. (1–30).

ERCIT, T.S. (1986): *The Simpsonite Paragenesis. The Crystal Chemistry and Geochemistry of Extreme Ta Fractionation.* Ph.D. thesis, Univ. of Manitoba, Winnipeg, Manitoba.

————, ČERNÝ, P. & HAWTHORNE, F.C. (1993): Cesstibtantite – a geologic introduction to the inverse pyrochlores. *Mineral. Petrol.* **48**, 235–255.

————, HAWTHORNE, F.C. & ČERNÝ, P. (1986): The crystal structure of bobfergusonite. *Can. Mineral.* **24**, 605–614.

EWING, R.C. & EHLMANN, A.J. (1974): Annealing study of metamict, orthorhombic, rare earth, AB_2O_6-type, Nb–Ta–Ti oxides. *Can. Mineral.* **13**, 1–7.

FOORD, E.E., SHARP, W.N. & ADAMS, J.W. (1984): Zinc- and Y-group-bearing senaite from St. Peters Dome, and new data on senaite from Dattas, Minas Gerais, Brazil. *Mineral. Mag.* **48**, 97–106.

GATEHOUSE, B.M., GREY, I.E. & KELLY, P.R. (1979): The crystal structure of davidite. *Am. Mineral.* **64**, 1010–1017.

GREY, I.E. & GATEHOUSE, B.M. (1978): The crystal structure of landauite, $Na[MnZn_2(Ti,Fe)_6Ti_{12}]O_{38}$. *Can. Mineral.* **16**, 63–68.

POPE, M.T. (1983): *Heteropoly and Isopoly Oxometallates.* Springer-Verlag, Berlin, Germany.

POUCHOU, J.L. & PICHOIR, F. (1991): Quantitative analysis of homogeneous or stratified microvolumes applying the model "PAP". *In* Electron Probe Quantitation (K.F.J. Heinrich & D.E. Newbury, eds.). Plenum Press, New York, N.Y. (31–75).